Optically detected magnetic-resonance study of triplet-state dynamics in C_{70}

P. A. Lane, X. Wei,* and Z. V. Vardeny
Department of Physics, University of Utah, Salt Lake City, Utah 84112

J. Partee and J. Shinar
Ames Laboratory–U.S. Department of Energy and Department of Physics and Astronomy, Iowa State University, Ames, Iowa 50011
(Received 15 September 1995)

We present studies of fluorescence, phosphorescence, photoinduced absorption, and their respective optically detected magnetic resonance of C_{70} molecules dispersed in polystyrene glasses. Two distinct triplet excitons are identified with principle zero-field splitting parameters ($D \approx 0.0089$ and 0.0098 cm^{-1}, respectively) almost twice those reported in the literature ($D \approx 0.0052$ cm^{-1}). The first triplet is axially symmetric ($E \approx 0$) and phosphorescent. Dramatic changes in the line shape and intensity of this triplet are observed as the temperature increases due to a dynamic Jahn-Teller effect. The second triplet, which is believed to arise from strained C_{70} molecules, has no axial symmetry ($E \approx D/3$) and is not phosphorescent.

Synthesis of macroscopic quantities of fullerenes[1] has stimulated intense theoretical and experimental studies of these novel allotropes of carbon. While initial attention focused on C_{60}, there has been increasing interest in C_{70}. The excited-state dynamics of C_{70} differ from C_{60}; it has much longer triplet lifetimes and is consequently phosphorescent. Excitations in C_{70} have been studied by photoluminescence (PL) spectroscopy,[2–7] triplet-state dynamics,[8–10] light-induced electron-spin resonance (LESR),[11–14] and optically detected magnetic resonance (ODMR).[15–19] Both fluorescence and phosphorescence bands have been observed. The fluorescence of C_{70} has been attributed to recombination of photoexcited singlets.[5,7–9] The phosphorescence, on the other hand, has been assigned to radiative decay of triplets generated by intersystem crossing.[2–6]

The major part of this work examines ODMR of C_{70} molecules isolated in polystyrene or toluene/polystyrene matrices (C_{70}:PS and C_{70}:T/PS, respectively), to elucidate the triplet spin dynamics. By separately monitoring the fluorescence-, phosphorescence-, and photoinduced absorption-detected magnetic resonance (FDMR, PhDMR, and PADMR, respectively), we have been able to identify two distinct triplet excitons in C_{70}. Triplet A (T_A) is phosphorescent, axially symmetric ($E \approx 0$), and dominates the low-temperature PL-quenching PhDMR spectrum, whereas triplet B (T_B) is nonradiative, has no axial symmetry ($E \approx D/3$), and dominates the PL-enhancing FDMR spectrum. Dramatic changes in the PhDMR line shape and intensity observed for T_A as the temperature increases are interpreted as a manifestation of a dynamic Jahn-Teller (JT) effect.[20] All ODMR spectra are >200 G wide, leading us to conclude that the zero-field splitting (ZFS) of the two triplets ($|D| \approx 0.0089$ and 0.0098 cm^{-1}, respectively) are much larger than previously thought ($|D| \approx 0.0052$ cm^{-1}).[11–15]

C_{70} powder of purity greater than 99.8% was purchased from Texas Fullerenes Corporation and dissolved in a 10% polystyrene/90% toluene solution at a concentration of 0.125 mg of C_{70} per ml. C_{70}:T/PS samples were degassed by multiple freeze-pump-thaw cycles and sealed in quartz tubes. C_{70}:PS samples were prepared by evaporating the toluene/polystyrene solution to form a translucent glass with $\sim 1\%$ C_{70} by weight. For PADMR measurements, the pump and probe beams constantly illuminate the sample mounted in a high-Q microwave cavity at 3 GHz. For PLDMR measurements, the sample was mounted in an X-band cavity at 9.35 GHz and excited at 488 nm by an Ar^+ laser. Resonant absorption of microwaves leads to small changes δT in the transmission T proportional to δn, the change in the density of photoexcitations, as well as small changes δI in the PL intensity I. The microwaves were amplitude modulated and phase-sensitive changes in T or I were detected by a photodiode.

The fluorescence, phosphorescence, and photoinduced absorption (PA) spectra of typical C_{70}:PS samples are shown in Fig. 1. Peaks in the relatively weak fluorescence spectrum are observed at 1.86, 1.79, and 1.72 eV, respectively, possibly due to a 70-meV vibronic progression or several independent false origins. The phosphorescence spectrum, on the other hand, is much sharper and more intense than the fluorescence, with strong peaks visible at 1.533, 1.490, 1.455, 1.394, and 1.346 eV, respectively, and weaker peaks at 1.31, 1.25, and 1.21 eV, respectively. The integrated phosphorescence was approximately 12 times as intense as the fluorescence. The PA spectrum at 4 K contains two intense bands: T_1 at 1.3 eV and T_2 at 1.8 eV, respectively. The intensity of both bands increases linearly with excitation power, showing monomolecular recombination kinetics.

Figure 2(a) shows the FDMR of a C_{70}:T/PS glass measured between 1.7 and 1.9 eV [within the fluorescence band, see Fig. 1(a)] at 20 K. The FDMR is PL enhancing and is symmetric about $g \approx 2$, with shoulders separated by 220 G and a relatively narrow peak at $g \approx 2$. This spectrum is characteristic of a triplet exciton (T_B) with ZFS parameters $|D| = 0.0098$ cm^{-1} (110 G) and $|E| \approx D/3$. The PhDMR [Fig. 2(b)] of a C_{70}:T/PS glass measured between 1.4 and 1.5 eV [within the phosphorescence band, see Fig. 1(b)] at 10 K, on the contrary, is notably asymmetric, consisting of two PL-quenching resonances split by ~ 95 G with the low-field resonance more intense than the high-field resonance. We assign this resonance to another triplet exciton (T_A) with

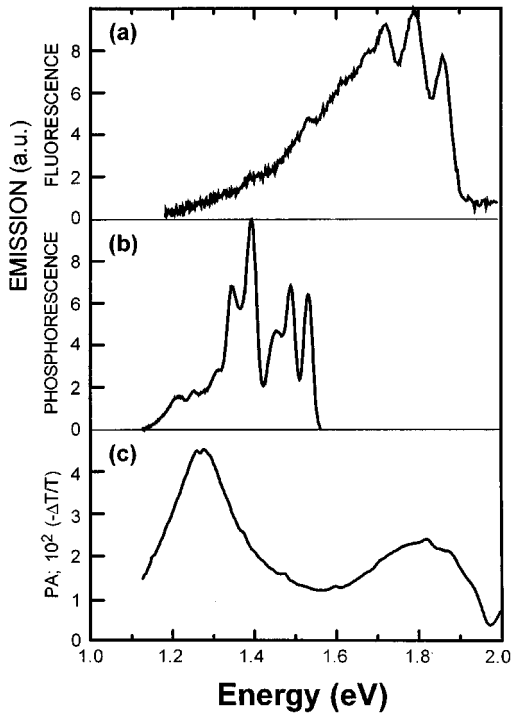

FIG. 1. (a) Fluorescence, (b) phosphorescence, and (c) photoinduced absorption of C_{70}:PS.

ZFS $|D|=0.0089\ \mathrm{cm}^{-1}$ (95 G) and $|E|=0$. Figure 2(c) shows the PADMR of a C_{70}:PS glass measured at 4 K with the probe wavelength fixed at 1.3 eV [at T_1, see Fig. 1(c)]. The PADMR is roughly symmetric about $g=2$ with a central peak, two sharp dips separated by ~100 G, and two shoulders separated by ~200 G. The spectrum of the PADMR, determined by varying the probe wavelength at a resonant

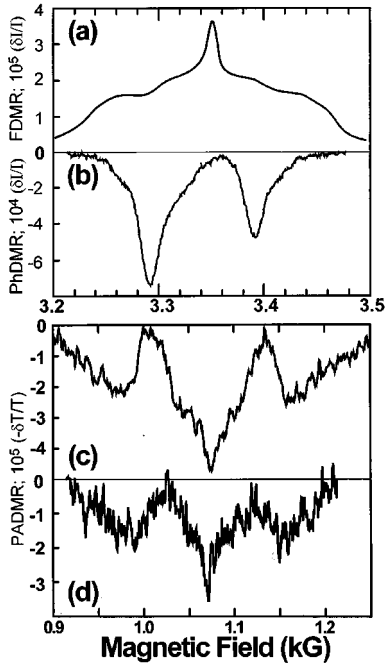

FIG. 2. (a) FDMR and (b) PhDMR spectra, respectively, of C_{70}:T/PS glasses at 20 K and 9.35 GHz. (c) Experimental and (d) simulated full-field PADMR spectra of C_{70}:PS at 10 K and 3.0 GHz.

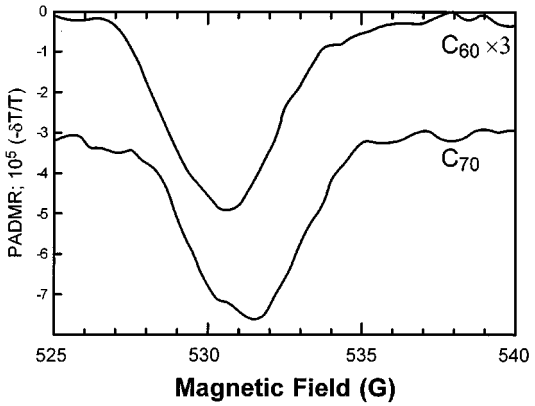

FIG. 3. Half-field PADMR spectra of C_{60}:PS and C_{70}:PS glasses at 10 K and 3.0 GHz.

field, is identical to that of the PA.[5] This leads us to conclude that the PA is due to triplet excitations. The PADMR can clearly be shown as due to both triplets by combining the FDMR and PhDMR with the appropriate weighting factor [Fig. 2(d)].

While the results of full-field LESR and ODMR measurements are ambiguous, the position of the half-field resonance due to $\Delta m_s=2$ transitions can definitively resolve the issue of ZFS parameters. For a triplet exciton, the intensity of the half-field resonance scales as $(D/h\nu)$.[21] Hence, while the half-field resonance has not been observed in measurements at 9 GHz, we have been able to observe the half-field resonance operating at 3 GHz. The half-field powder pattern of a triplet exciton diverges at $H=\frac{1}{2}\sqrt{H_0^2-(D+E)^2}$,[21] where $H_0=1068$ G in our measurements. The widely accepted ZFS for C_{60} (Ref. 19) predict a divergence at 530.5 G, in fairly good agreement with the experimental results shown in Fig. 3. The generally accepted ZFS for C_{70} ($D=56$ G, $E=7$ G)[11–15] predict a resonance at 533.1 G, whereas for $D=95$ G and $E=0$, we predict a resonance at 531.9. The actual half-field resonance, shown in Fig. 3, is strongest at 531.6 G, in good agreement with the latter parameters. The different D in C_{60} and C_{70} can be understood as due to the different sizes of the respective molecules. C_{60} is 7.1 Å in diameter and the two axes of C_{70} are 6.9 and 7.9 Å, respectively. As $D\sim r^{-1/3}$, where r is the radius of the exciton, this leads to the relationship $D_{C_{70}}\approx D_{C_{60}}\sqrt[3]{r_{C_{60}}/r_{C_{70}}}$. From this rough approximation, one would expect that purely from size considerations, $D_{C_{70}}\approx 90$ G.

We next turn to the intriguing dynamics of triplet A. The PhDMR of C_{70}:T/PS measured between 5 and 80 K with the microwaves modulated at 26 Hz is shown in Fig. 4. At 5 K, the powder pattern consists of two PL-quenching resonances split by ~110 G. The splitting of the resonances is roughly similar to the features seen in the PADMR powder pattern [Fig. 2(c)]. However, as the temperature increases, a phosphorescence-enhancing component emerges and the high-field quenching resonance weakens and vanishes. At 80 K, the powder pattern is strikingly antisymmetric. The resonance intensity rapidly decreases as the temperature increases, disappearing above 80 K.

To interpret the various full-field powder patterns, we consider the following triplet spin Hamiltonian $\mathscr{H}$:[21]

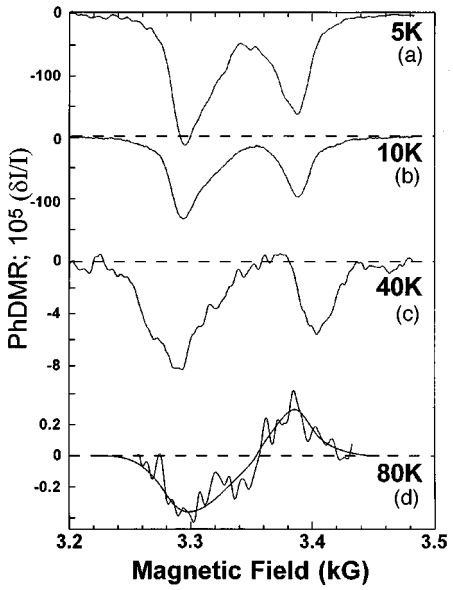

FIG. 4. PhDMR of a C_{70}:T/PS glass between 5 and 80 K. The line at 80 K is to guide the eye.

$$\mathscr{H}=g\mu_B\mathbf{H}\cdot\mathbf{S}+D(S_z^2-\tfrac{1}{3}S^2)+E(S_y^2-S_x^2), \qquad (1)$$

where $\mathbf{H}$ is the magnetic field and the ZFS parameters D and E in reduced coordinates are $D=\frac{3}{4}g^2\mu_B^2\langle(r^2-3z^2)/r^5\rangle$ and $E=\frac{3}{4}g^2\mu_B^2\langle(y^2-x^2)/r^5\rangle$, respectively. If $E\approx 0$, the x and y axes are equivalent and, hence, the triplet is axially symmetric. The ODMR spectrum is determined by three distinct zero-field sublevels $|x\rangle$, $|y\rangle$, and $|z\rangle$, which correspond to the principal axes of the triplet. Under a strong magnetic field, the three eigenfunctions $|1\rangle$, $|0\rangle$, and $|-1\rangle$ can be expressed in terms of the zero-field sublevels $|i\rangle=c_{ix}|x\rangle+c_{iy}|y\rangle+c_{iz}|z\rangle$, where the coefficients c_{ij} are functions of the applied field and triplet orientation relative to the field.[21,22] Magnetic resonance transitions occur when the splitting between two triplet sublevels is equal to $h\nu$. For a single triplet, there are usually three resonances, corresponding to two $\Delta m_s=1$ transitions and one $\Delta m_s=2$ transition. For isotropic samples, however, the triplets are randomly oriented and the magnetic resonance spectra is an average over all possible orientations, forming two powder patterns; one for $\Delta m_s=2$ (half field) and the other for $\Delta m_s=1$ (full field). The full-field powder pattern of an axially symmetric ($E\approx 0$) triplet will contain singularities at $H_0\pm D/2$, respectively, and steps at $H_0\pm D$, respectively, where $g\mu_B H_0=h\nu$.[22,23] A triplet with no axial symmetry ($E\approx D/3$) results in a full-field powder pattern with a central singularity at H_0 and shoulders at $H_0\pm D$.[20,21]

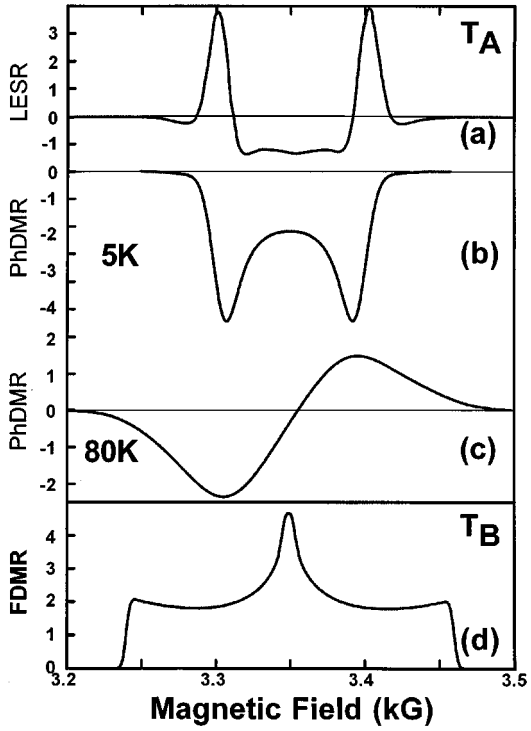

FIG. 5. Calculated powder patterns for triplet A: (a) LESR, (b) PhDMR at 5 K, (c) PhDMR at 80 K. (d) Calculated FDMR powder pattern of triplet B.

At resonance and under microwave saturation, the populations of two spin sublevels coupled by magnetic resonance are equalized. Hence, the ADMR signal is proportional to the difference in level population (spin polarization) in the absence of magnetic resonance.[22] In order to model a powder pattern, the Hamiltonian in Eq. (1) must be solved and the spin polarization calculated. We take the respective generation and recombination rates for the high-field triplet sublevels to be $G_i=|c_{ix}|^2G_x+|c_{iy}|^2G_y+|c_{iz}|^2G_z$ and $R_i=|c_{ix}|^2R_x+|c_{iy}|^2R_y+|c_{iz}|^2R_z$, where $G_{x,y,z}$ and $R_{x,y,z}$ are the respective generation and recombination rates of the zero-field triplet sublevels. A unique radiative transition rate R' is given for each triplet sublevel. The possibility of transitions between triplet sublevels (spin-lattice relaxation) is also included in our model. Taking all these factors into account, the rate equation for each triplet sublevel is

$$dn_i/dt=n_iR_i-S(n_i-n_{iB})-G_i, \qquad (2)$$

where n_{iB} satisfy the Boltzmann distribution and G, R, and S are the relative generation, recombination, and spin-lattice relaxation rates. Under steady-state conditions, $dn_i/dt=0$, leading to a set of three coupled equations, whose solution gives the steady-state sublevel populations.

Using the above model, we have successfully reproduced in Figs. 5(a)–5(c) spectra of the LESR (Ref. 12) and PhDMR of T_A at 5 K [Fig. 4(a)] as well as the antisymmetric PhDMR detected at 80 K [Fig. 4(d)]. We note the absence of steps at $H_0\pm D$ in the PhDMR of T_A. These steps are due to triplets where the magnetic field is parallel to their z axis. The respective triplet sublevel populations for $\mathbf{H}\|z$, absent spin-lattice relaxation, are

$$n_1=\frac{G_x+G_y}{R_x+R_y}, \quad n_0=\frac{G_z}{R_z}, \quad n_{-1}=\frac{G_x+G_y}{R_x+R_y}. \qquad (3)$$

If the generation and recombination rates of the triplet in zero field are such that $n_1\cong n_0\cong n_{-1}$ for $\mathbf{H}\|z$, then these steps do not appear in the powder pattern. Instead, there is a gradual onset of the resonance. If a LESR technique is used that produces derivative spectra, the onset of the triplet will be masked, leading to a mistakenly low value of D. We believe this to be the case for previous studies of C_{70}.[11–15] The generation (G), recombination (R), and radiative transition (R') rates for triplet A are shown in Table I. For these calculations S was set at 0.05.

In order to model the PhDMR temperature dependence, we have considered the possibility that a dynamic Jahn-Teller effect might lead to a mixing of the character of the x and y zero-field sublevels as a consequence of hopping among equivalent JT deformations symmetrically surrounding the C_{70} principal axis z. Then, for the above set of generation and recombination parameters, magnetic resonance will decrease the decay of triplets for **H**‖**x** and increase the rate of decay for triplets with **H**‖**y**. The observed PL-quenching PhDMR for $T<20$ K requires that the PhDMR spectrum is dominated by triplets with **H**‖**x**. At higher temperatures, Jahn-Teller mixing results in nearly equal contributions from both sublevels, leading to an antisymmetric PhDMR spectrum (Fig. 4). The chosen set of generation, recombination, and radiative transition probabilities must be chosen such that spin polarization vanishes for **H**‖**z**, the low-temperature PhDMR is dominated by emission from one sublevel, and nearly equal cancellation of contributions from the $|x\rangle$ and $|y\rangle$ sublevels at high T [as in Fig. 5(c)]. The discovery of a dynamic Jahn-Teller effect in C_{60} has led to suggestions that this effect may be linked to superconductivity in alkali-doped C_{60}.[23,24] Given that we find evidence for such an effect in C_{70}, this scenario should be revised accordingly.

The powder pattern of T_B is seen in both the full-field PADMR and FDMR powder patterns (Fig. 2). The absence of this triplet in the PhDMR spectrum indicates that emission from this triplet is forbidden. The powder pattern of the triplet observed in FDMR can be easily simulated by a triplet with $D=0.0098$ cm^{-1} and $E\approx D/3$ [Fig. 5(d)]. The complete departure from axial symmetry coupled with the absence of phosphorescence suggests that it resides on distorted molecules, possibly due to strain in the T/PS matrix. This leads us to suggest that fluorescence from C_{70} is defect related, which is consistent with the observation of fluorescence from X traps in C_{60}.[25] We can then conclude that the FDMR of T_B is due to enhanced nonradiative decay to the ground state, so-called "ground-state recovery."[26,27] The PADMR of T_B is due to transitions between triplet sublevels, which increases the rate of decay to the ground state. Consequently, the photoinduced absorption is reduced and a negative PADMR is detected ($\delta n_T<0$). Enhanced decay back to the ground state results in increased absorption of the laser excitation and, hence, greater fluorescence. Fluorescence will be seen only from distorted molecules and this distortion is evidenced by the loss of axial symmetry of T_B.

TABLE I. Generation, recombination, and radiative recombination rates used to calculate LESR and PhDMR spectra displayed in Fig. 5.

	Parameter	X	Y	Z
5 K [Figs. 5(a) and 5(b)]	G	0.53	0.27	0.2
	R	0.27	0.53	0.2
	R'	0.235	0.21	0.04
80 K [Fig. 5(c)]	G	0.252	0.248	0.1
	R	0.248	0.252	0.1
	R'	0.124	0.131	0.02

In conclusion, we have examined triplet-state dynamics of C_{70} by three ODMR spectroscopies. Two distinct triplet excitons have been observed: Triplet A is axially symmetric, responsible for phosphorescence and resides on undistorted molecules. Triplet B has no axial symmetry, is nonradiative, and possibly due to strain in the matrix. The FDMR is due to ground-state recovery of the T_B whereas the PhDMR is due to magnetic resonance effects on the direct radiative recombination of T_A. The unusual dynamics of T_A have been attributed to a dynamic Jahn-Teller effect. The ZFS parameters of these triplets are much larger than previously thought due to unique generation and recombination rates, which mask the overall width of the powder pattern.

The work at the University of Utah was supported by DOE FG-03-93ER45490. Ames Laboratory is operated by Iowa State University for the U.S. Department of Energy under Contract No. W-7405-Eng-82. The work at Iowa State University was supported by the Director for Energy Research, Office of Basic Energy Sciences, USDOE.

*Present address: Los Alamos National Laboratory, Albequerque, NM 87545.

[1] W. Krätschmer *et al.*, Nature **347**, 354 (1990).
[2] S. P. Sibley *et al.*, Chem. Phys. Lett. **188**, 187 (1992).
[3] Y. Wang, J. Phys. Chem. **96**, 764 (1992).
[4] J. W. Arbogast and C. S. Foote, J. Am. Chem. Soc. **113**, 8886 (1991).
[5] E. Shin *et al.*, Chem. Phys. Lett. **209**, 427 (1993).
[6] D. Kim *et al.*, J. Am. Chem. Soc. **114**, 4429 (1992).
[7] R. E. Haufler *et al.*, Chem. Phys. Lett. **179**, 449 (1991).
[8] R. W. Williams and J. W. Verhoeven, Chem. Phys. Lett. **194**, 446 (1992).
[9] K. Tanigaki *et al.*, Chem. Phys. Lett. **185**, 189 (1991).
[10] M. R. Fraelich and R. B. Weisman, J. Phys. Chem. **97**, 11 145 (1993).
[11] M. Terazima *et al.*, J. Phys. Chem. **97**, 5447 (1993).
[12] M. R. Wasielewski *et al.*, J. Am. Chem. Soc. **113**, 2774 (1991).
[13] H. Levanon *et al.*, J. Am. Chem. Soc. **115**, 8722 (1993).
[14] M. Terazima *et al.*, Chem. Phys. Lett. **195**, 333 (1992).
[15] X. Wei *et al.*, Solid State Commun. **85**, 455 (1993).
[16] X. Wei *et al.*, Synth. Met. **54**, 273 (1993).
[17] P. A. Lane and J. Shinar, Phys. Rev. B **51**, 10 028 (1995).
[18] X. Wei and Z. V. Vardeny, Mol. Cryst. Liq. Cryst. **256**, 307 (1994).
[19] P. A. Lane *et al.*, Phys. Rev. Lett. **68**, 887 (1992).
[20] X. Wei and Z. V. Vardeny, Phys. Rev. B **52**, R2317 (1995).
[21] C. P. Poole, *Electron Spin Resonance* (Wiley, New York, 1983).
[22] X. Wei, Ph.D. thesis, University of Utah, 1992.
[23] M. Schluter *et al.*, Phys. Rev. Lett. **68**, 526 (1992).
[24] A. Auerbach, Phys. Rev. Lett. **72**, 2931 (1994).
[25] W. Guss *et al.*, Phys. Rev. Lett. **72**, 2644 (1994).
[26] R. A. Street, Phys. Rev. B **26**, 3588 (1982); F. Boulitrop, *ibid*. **28**, 6192 (1983).
[27] R. H. Clarke, *Triplet State ODMR Spectroscopy* (Wiley, New York, 1982), Chap. 2.